Electronic Supplementary Information for

Stop and restart of polycondensation reactions of highly reactive sol–gel precursors for nanoscale surface molding

Norihiro Mizoshita* and Yuri Yamada

Contents

1. Experimental section

1.1. Materials and methods

All reagents and solvents were purchased from Aldrich, FUJIFILM Wako Pure Chemical, Gelest, or Tokyo Chemical Industry and used without further purification. Syntheses of compounds **1a** and **1c** were described in our previous reports.[1,2] ^{1}H and ^{13}C NMR spectra were measured using a JEOL JNM-ECX400P spectrometer. ^{29}Si NMR spectra were measured using a JEOL JNM-ECA500 spectrometer. The chemical shifts for all spectra were referenced to tetramethylsilane at 0 ppm. Infrared measurements were conducted with a Thermo Nicolet Avatar 360 FT-IR spectrometer using an attenuated total reflection (ATR) attachment. Matrix-assisted laser desorption/ionization (MALDI) time-of-flight mass spectra were recorded on a Bruker Daltonics autoflex maX (laser wavelength: 355 nm) mass spectrometer.

Solid-state [29]Si magic-angle spinning (MAS) and ^{13}C cross-polarization (CP) MAS NMR spectra were recorded on a Bruker Avance 400 spectrometer (at 79.49 MHz for [29]Si and 100.62 MHz for ^{13}C) using 7 mm zirconia rotors and a sample spinning frequency of 4 kHz. The chemical shifts for all spectra were referenced to tetramethylsilane at 0 ppm. For ^{29}Si MAS NMR measurements, single 4.5-μs $\pi/2$ pulses were applied with proton decoupling during detection, 60-s recycle delays, and 900 scans in order to ensure complete relaxation of [29]Si magnetization for all silicate species between each signal acquisition. ^{13}C CP MAS NMR spectra were acquired using a CP pulse sequence with $\pi/2$ pulses of 4.5 μs, CP contact times of 1.75 ms, proton decoupling during detection, 5-s recycle delays, and 2000 scans.

AFM observation was performed at room temperature by using the dynamic force mode on a NanoNavi E-sweep scanning probe microscope system (Hitachi). All images were collected by using a 20-μm scanner and a cantilever SI-DF20 (radius of Si tip: 10 nm, spring constant: 15.0 N m^{-1}, resonance frequency: 131 kHz). All of the measurements were performed in ambient air, and height images were recorded with 256×256-pixel resolution. The AFM images were scanned at scanning frequencies of 0.78–0.94 Hz and collected at scales of 10×10, 5×5, and 2×2 μm.

X-ray diffraction (XRD) measurements were performed on a Rigaku RINT-TTR diffractometer using Cu-Kα radiation (50 kV, 300 mA).
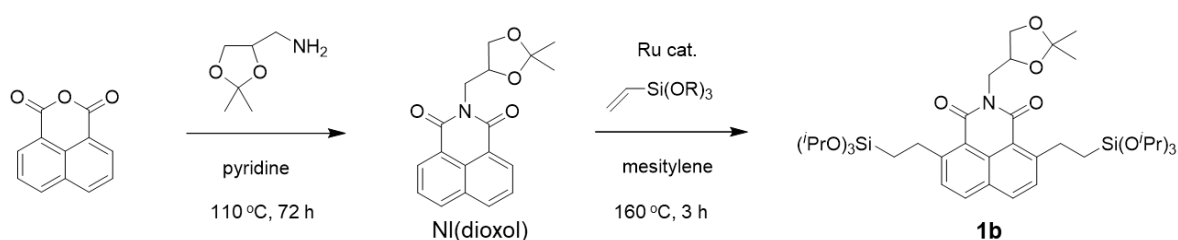
1.2. Synthesis of 1b

Compound **1b** was synthesized according to Scheme S1. The NMR spectra of **1b** are shown in Figs. S1 and S2.

Synthesis of N-[(2,2-dimethyl-1,3-dioxolan-4-yl)methyl]-1,8-naphthalimide (NI(dioxol)): A mixture of 1,8-naphthalic anhydride (2.97 g, 15.0 mmol), 2,2-dimethyl-1,3-dioxolane-4-methanamine 3.28 g, 25.0 mmol), and pyridine (20 mL) was stirred at 110 °C for 72 h under nitrogen atmosphere. After cooling to room temperature,

water (150 mL) was added and the mixture was stirred for 0.5 h. The resultant precipitate was collected by suction filtration. The solid material was dissolved in acetonitrile and reprecipitated by addition water. The precipitate was collected by suction filtration, washed thoroughly with water, and dried in vacuo to afford the product as an off-white solid in 92% yield (4.30 g). ^{1}H NMR (400 MHz, CDCl$_3$, δ in ppm): 1.34 (s, 3H; -CH_3), 1.49 (s, 3H; -CH_3), 3.92 (m, 1H), 4.11 (m, 1H), 4.21 (m, 1H), 4.52–4.62 (m, 2H), 7.76 (m, 2H; Ar-H), 8.22 (m, 2H; Ar-H), 8.62 (m, 2H; Ar-H).

Synthesis of 1b: A mixture of NI(dioxol) (2.00 g, 6.42 mmol) and RuH$_2$(CO)(PPh$_3$)$_3$ (165 mg, 0.18 mmol) was dissolved in mesitylene (50 mL) at 100 °C under nitrogen atmosphere. Triisopropoxyvinylsilane (5.81 g, 25.0 mmol) was added to the solution and the reaction mixture was stirred at 160 °C for 3 h. After cooling to room temperature, the mixture was purified by silica gel column chromatography using eluents of hexane/chloroform = 1/1 (v/v) and chloroform/ethanol = 10/1 (v/v). The crude product obtained as a purple solid. To remove the residual Ru derivatives, the crude material dissolved in chloroform (150 mL) was stirred with a scavenger, SiliCycle SiliaMetS® DMT (15.0 g), for 24 h. The scavenger was removed by suction filtration and the filtrate was dried using a rotary evaporator and vacuum dryer to afford the product as a pale red viscous oil in 100% yield (4.98 g). The product gradually crystallizes at room temperature. ^{1}H NMR (400 MHz, CDCl$_3$, δ in ppm): 1.06 (m, 4H; -CH_2-Si), 1.24 (d, J = 6.3 Hz, 36H; Si-O-CH(CH_3)$_2$), 1.34 (s, 3H; -CH_3), 1.49 (s, 3H; -CH_3), 3.51 (m, 4H; Ar-CH_2-), 3.93 (m, 1H), 4.06 (m, 1H), 4.21 (m, 1H), 4.31 (sep, J = 6.3 Hz, 6H; Si-O-CH(CH$_3$)$_2$), 4.51 (m, 1H), 4.63 (m, 1H), 7.54 (d, J = 8.3 Hz, 2H; Ar-H), 7.99 (d, J = 8.3 Hz, 2H; Ar-H). ^{13}C NMR (100 MHz, CDCl$_3$, δ in ppm): 13.3, 25.6, 25.8, 26.8, 30.3, 42.6, 65.0, 68.2, 74.0, 109.2, 118.3, 129.3, 130.4, 133.4, 153.6, 163.9. IR (ATR): 763, 853, 872, 885, 1027, 1118, 1172, 1333, 1368, 1379, 1449, 1555, 1658, 1695, 2886, 2934, 2970 cm^{-1}. MS (MALDI) m/z : [M − H]$^+$ calcd for C$_{40}$H$_{65}$NO$_{10}$Si$_2$, 774.4; found 774.2.

Scheme S1 Synthesis of **1b**.
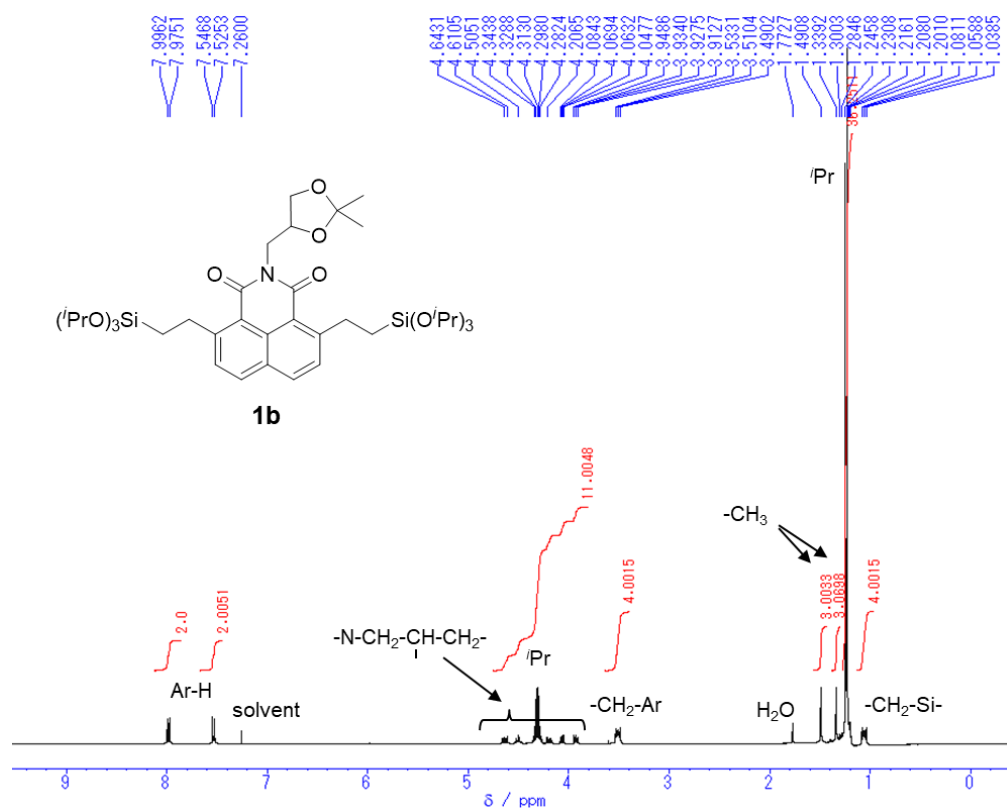
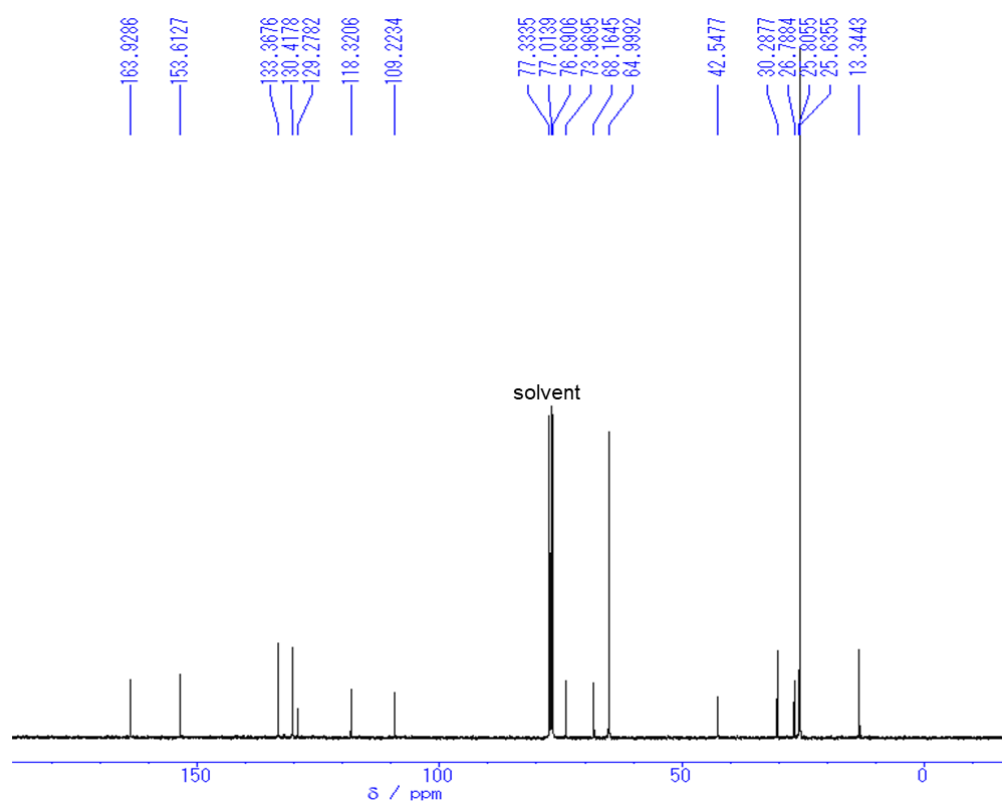**Fig. S1**　^{1}H NMR spectrum of **1b** in a CDCl$_3$ solution.

Fig. S2　^{13}C NMR spectrum of **1b** in a CDCl$_3$ solution.

1.3. Preparation of organosilica films

SG method: Organosilane precursor **1** (90 mg) was dissolved in ethanol (1.0 mL). After adding 2 M hydrochloric acid (12 µL), the solution was stirred at room temperature for 30 min. The sol solution was spin-coated onto silicon wafers at 1500 rpm for 8 s. The film was annealed at 80 °C for 1 h.

TE/A method: Organosilane precursor **1** (90 mg) was mixed with 2-ME (1.0 mL) and TsOH·H_2O (2 mg). The mixture in a sealed vessel was heated on a hot plate at 130 °C for 15 min, resulting in a homogeneous solution. After cooling to room temperature, triethylamine (10 µL) was added to the mixture and the precursor solution was spin-coated onto silicon wafers at 1500 rpm for 8 s. The resulting fluid film was cured by heating at 80–100 °C for 1–60 min.

Nanoimprinted organosilica films were prepared by pressing the following polymer molds (molds I–IV) onto the fresh spin-coated films (thickness: 250–300 nm) at 6–12 MPa. After annealing at 80 °C for 60 min (SG method) or at 80 °C for 3–60 min (TE/A method), the mold was removed.

>   Mold I: Soken FleFimo® PIP70-250, with a nanopillar array (diameter: 145 ± 30 nm, height: 250 ± 30 nm, pitch: 250 ± 30 nm)
>
>   Mold II: Soken FleFimo® PIP70-450, with a nanopillar array (diameter: 270 ± 50 nm, height: 200 ± 40 nm, pitch: 460 ± 30 nm)
>
>   Mold III: Soken FleFimo® LSP70-140, with a line-and-space pattern (line width: 70 ± 20 nm, height: 150 ± 30 nm, pitch: 140 ± 30 nm)
>
>   Mold IV: Soken FleFimo® HOP70-450, with a nanohole array (diameter: 240 ± 30 nm, height: 200 ± 40 nm, pitch: 460 ± 30 nm)

Organosilica films based on **2** and **3** were prepared by the same procedures with those used for **1**.

1.4. Preparation of metal oxide films (TE/A method)

Metal alkoxide precursors (Ti(OBu)$_4$, Zr(O^{i}Pr)$_4$ (70% in 1-propanol), Ge(O^{i}Pr)$_4$; 100 µL) were mixed with 2-ME (1.0 mL) and TsOH·H_2O (2.0 mg). The mixtures in sealed vessels were heated on a hot plate at 130 °C for 15 min, resulting in homogeneous solutions. After cooling to room temperature, triethylamine (10 µL) was added to the mixtures and the precursor solutions were spin-coated onto silicon wafers at 1800 rpm for 5 s. The resulting films were cured by heating at 100 °C for 60–120 min.

Nanoimprinted metal oxide films were prepared by the same procedures with those used for the organosilica films.

These metal oxide films were calcined at 550 °C for 4 h to crystallize the inorganic framework.

2. Structures and characterizations of the organosilica films

2.1. Transesterification, polycondensation and nanoimprinting

Fig. S3 shows ^{29}Si NMR spectra of reaction mixtures prepared using **1c** (see Fig. 2b) and the assignment of chemical shifts to the chemical structures of the silyl groups.
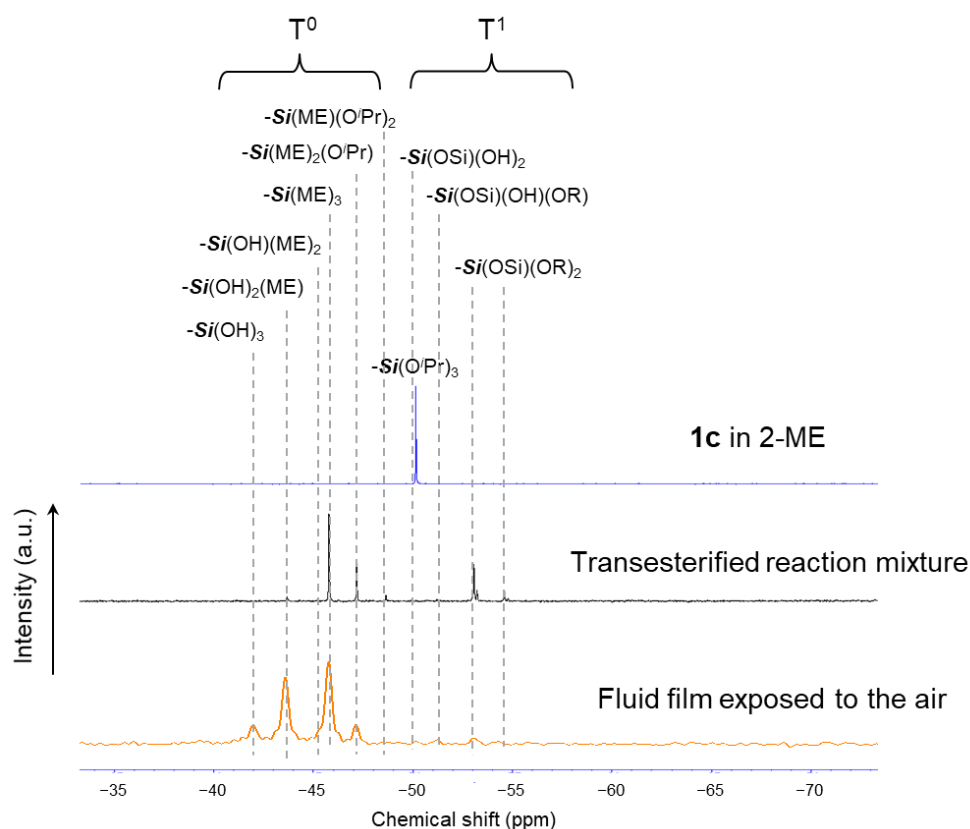

Fig. S3 Assignment of ^{29}Si NMR signals of reaction mixtures prepared using **1c**.

Fig. S4 shows ^{1}H NMR spectra of the transesterified reaction mixtures prepared using **1c**. Spectrum A is the ^{1}H NMR spectrum of the reaction mixture corresponding to that shown in Fig. 2b (B). ^{1}H NMR measurement was also carried out for a reaction mixture prepared under the condition of Si-O^{i}Pr/2-ME = 1/10 (molar ratio) to clarify the assignment of the signals (spectrum B). The progress of the transesterification reaction of **1c** was confirmed from these spectra as well as ^{29}Si NMR spectra.
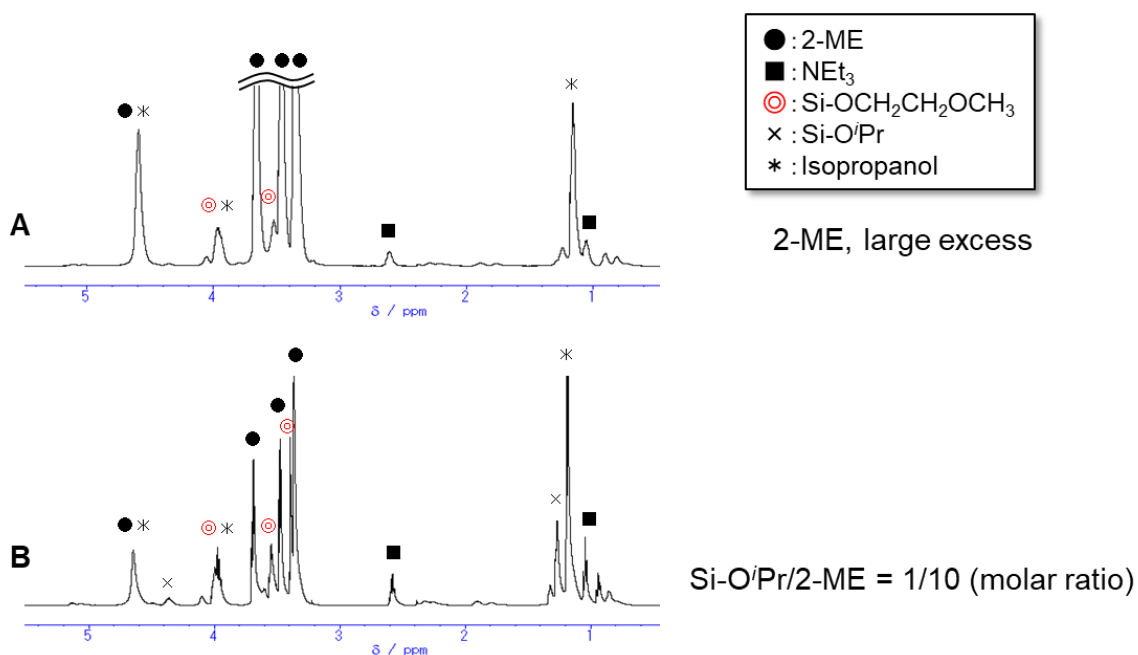
Legend:
● : 2-ME
■ : NEt$_3$
◎ : Si-OCH$_2$CH$_2$OCH$_3$
× : Si-O^{i}Pr
∗ : Isopropanol

A: 2-ME, large excess

B: Si-O^{i}Pr/2-ME = 1/10 (molar ratio)

Fig. S4 Assignment of ^{1}H NMR signals of transesterified reaction mixtures prepared using **1c**: (A) using large excess of 2-ME; (B) Si-O^{i}Pr/2-ME = 1/10 (molar ratio).

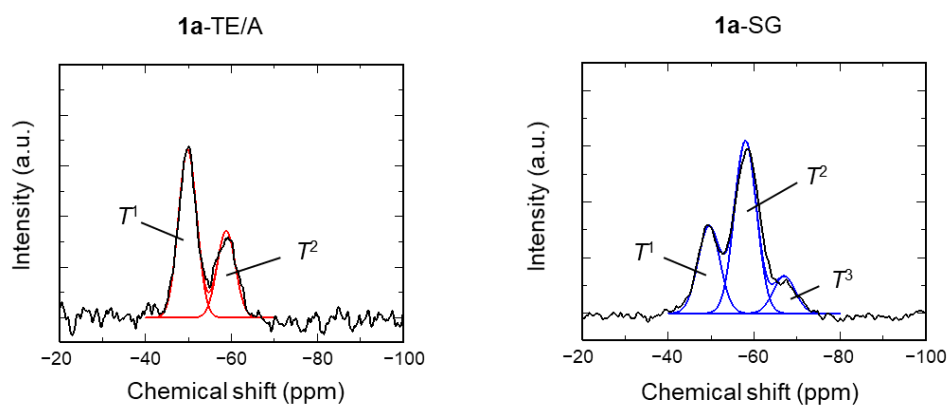Fig. S5 shows examples of the peak separation of signals in ^{29}Si MAS NMR spectra of organosilicas to calculate the degree of condensation (DC).

Fig. S5 Peak separation of the ^{29}Si MAS NMR spectra of organosilicas prepared from **1a**.

The value of DC was calculated using the following equation:

$$[DC]\,(\%) = \frac{1}{3}\,\frac{T^1 + 2\,T^2 + 3\,T^3}{\Sigma\,T} \times 100$$

where T^n is the peak area of the T^n signal. The DC of **1**-SG is 55–61%, whereas that of **1**-TE/A is 43–48%.

Fig. S6 shows supplementary AFM images of the nanoimprinted **1a**-TE/A, **1b**-TE/A, and **1b**-SG films. The nanohole array structure of **1a**-TE/A is similar to that of **1b**-TE/A shown in Figure 1c. The long-range periodicity of the well-oriented nanoporous structures was confirmed for the **1a**-TE/A and **1b**-TE/A films by the AFM observation. As mentioned in the main manuscript, nanoimprinting for the **1b**-SG film was unsuccessful.
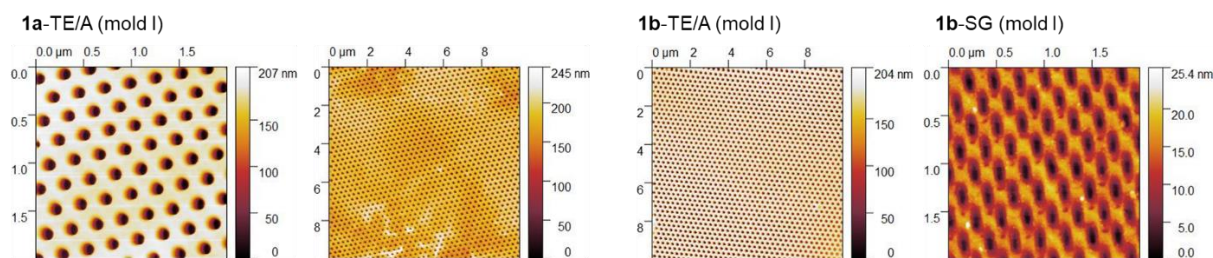

Fig. S6   AFM images of nanoimprinted **1a**-TE/A, **1b**-TE/A, and **1b**-SG films (prepared using mold I).

Moreover, we applied the nanoscale surface molding using the TE/A method to other organosilica films prepared from highly reactive precursors (**2** and **3**)[3,4] with large aromatic moieties (Fig. 3 and Fig. S7). The nanoimprinting of **2**-TE/A and **3**-TE/A films using mold I was successful and vertically oriented nanoporous films with long-range periodicity were obtained (Fig. S7). When the organosilica films were prepared using conventional SG method, the **2**-SG and **3**-SG films were hardened immediately after spin-coating and structural transfer from the mold surface to the organosilica films was unsuccessful (Fig. 3).
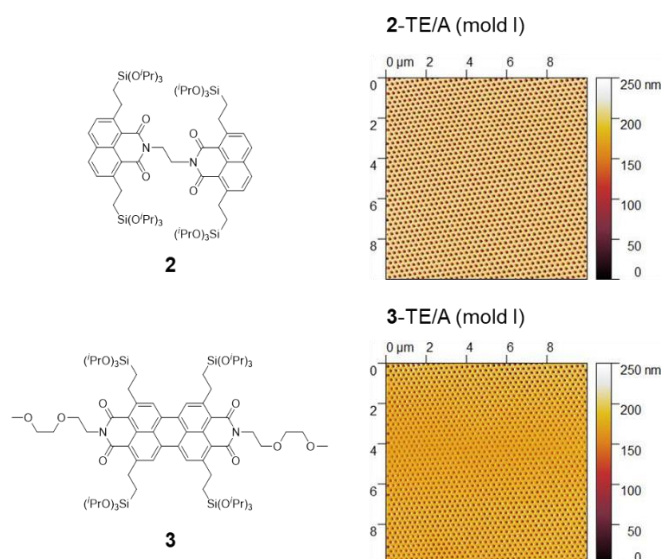
Fig. S7 AFM images (10×10 μm) of nanoimprinted **2**-TE/A and **3**-TE/A films (prepared using mold I).

As described in the main text, the TE/A method can be carried out using different reagents with similar roles to 2-ME, TsOH and NEt₃. Fig. S8 shows examples of nanoimprinting of naphthalimide-silica films prepared by modified TE/A methods.
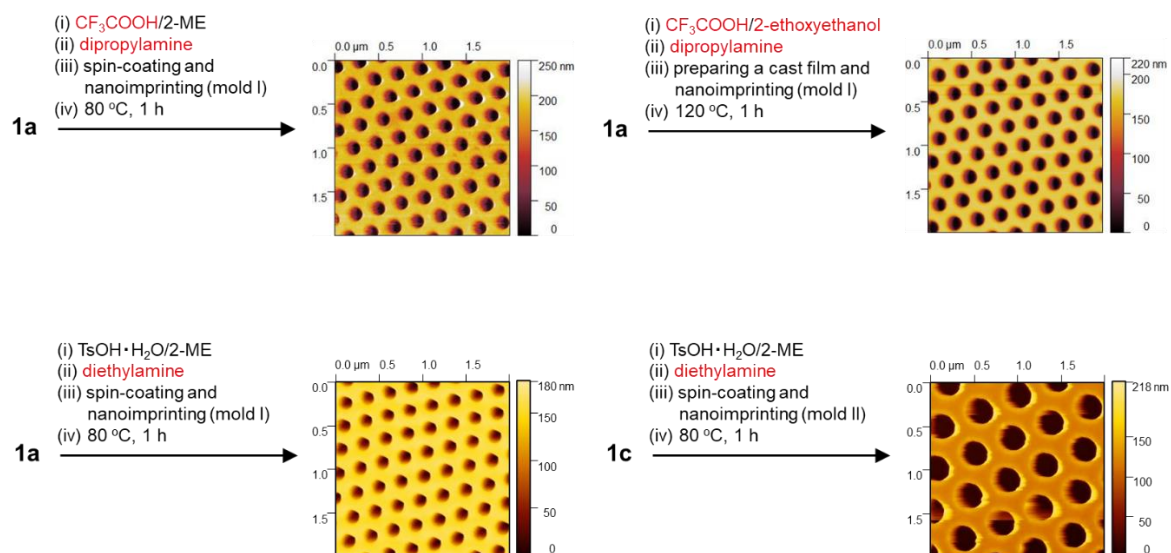

Fig. S8 AFM images of nanoimprinted naphthalimide-silica films prepared by modified TE/A methods.

The DCs of the organosilica frameworks prepared by the TE/A method are lower than those of **1**-SG due to the weak acidity of $HN^+Et_3 \cdot TsO^-$. The crosslinking of the framework can be promoted by post-treatments such as exposure to hydrochloric acid vapor after curing. For **1c**-TE/A, the DC increased from 48% to 65% by exposure to a vapor of 2 M hydrochloric acid (Fig. S9).
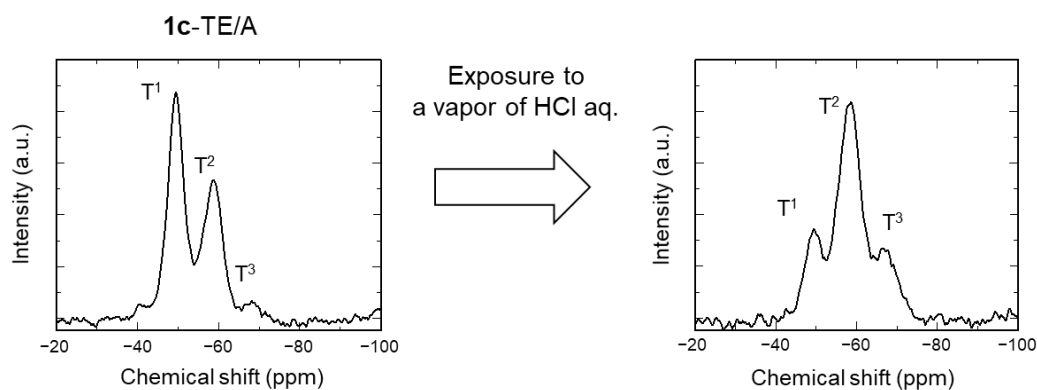

Fig. S9 Solid-state ^{29}Si MAS NMR spectra of **1c**-TE/A before and after exposure to a vapor of 2 M hydrochloric acid (100 °C, 3 h).

2.2. Deprotection of acetal group of 1b

The acetal protection group of **1b** is easily deprotected in the presence of acid catalysts and a diol group is formed. Fig. S10 shows the ^1H NMR spectra of NI(dioxol) before and after treatment with an acidic organic solution whose composition is similar to that of the sol solution in the SG method. The NMR signals corresponding to the dimethyl groups (1.33 and 1.49 ppm) completely disappeared after 2 h, indicating that acidic condition used in the SG method is sufficient for the deprotection of the acetal group.
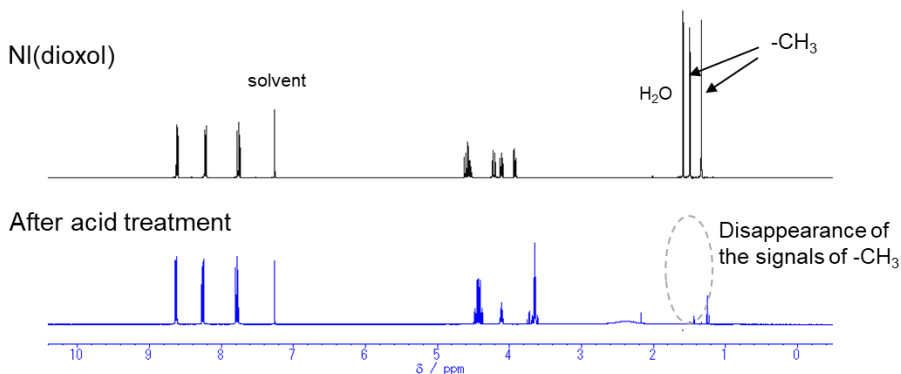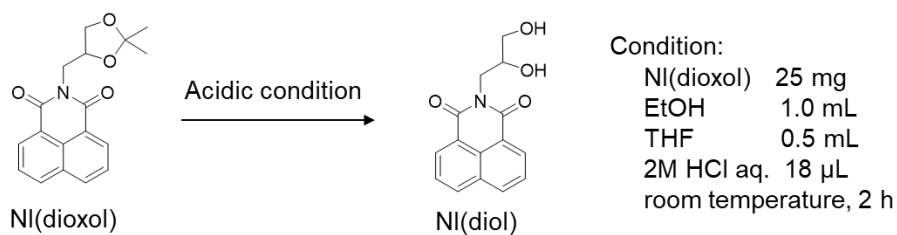
Fig. S10 ^{1}H NMR spectra of NI(dioxol) and the product after treatment with an acidic solution exhibiting acidity comparable to the sol mixtures in the SG method (in CDCl$_3$ solutions).

On the other hand, the reaction mixtures in the TE/A method contain smaller amounts of acid catalyst and water and the transesterification reaction is carried out in 15 min. ^{13}C CP-MAS spectra of NI(dioxol) and **1b**-TE/A showed that acetal protection groups were left in the **1b**-TE/A (Fig. S11). However, the degree of deprotection cannot be estimated from ^{13}C NMR spectra. We tried to directly measure the ^{1}H NMR spectrum of the precursor solution of the TE/A method. As a result, the residual amount of the protecting group was estimated to be 50–60% from the integrated values of the signals at 1.33 and 1.49 ppm and those of aromatic protons (Fig. S12). The deprotection reaction of **1b** turned out to progress partially in the TE/A method.
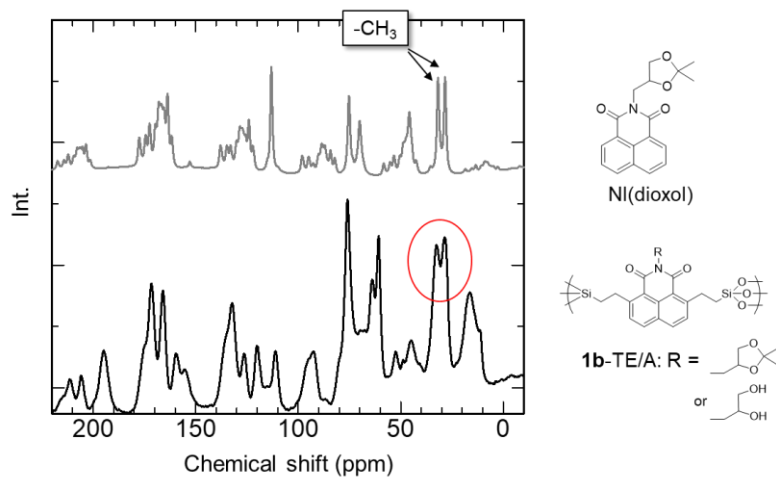
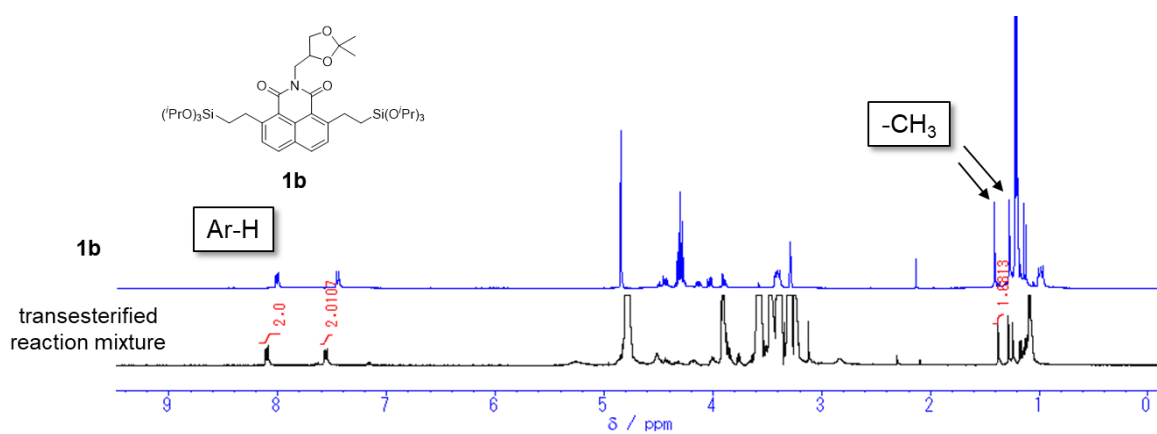**Fig. S11** ^{13}C CP-MAS NMR spectra of NI(dioxol) and **1b**-TE/A.

Fig. S12 ^{1}H NMR spectra of **1b** and the transesterified reaction mixture used for preparing **1b**-TE/A (in CD$_3$OD solutions).

3. Properties of catalysts

In the TE/A method, compounds that may catalyze the polycondensation reaction include triethylamine, TsOH·H_2O, and the salt HN^+Et_3·TsO^-. Fig. S13 shows IR spectra of these compounds. The salt was prepared by 1:1 mixture of triethylamine and TsOH·H_2O. The salt showed no decomposition for thermal annealing at 100 °C for 2 h.
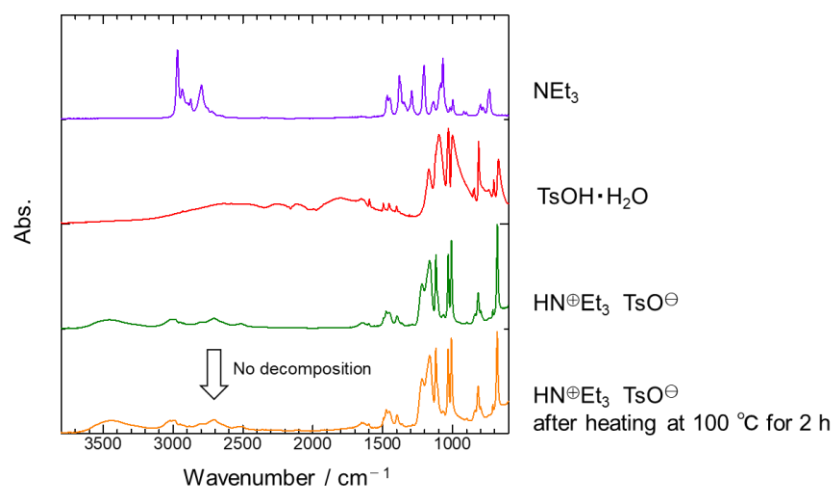

Fig. S13 IR spectra of NEt₃, TsOH·H_2O, and the mixture of them.

The pH values of 5 wt% aqueous solutions of NEt₃, TsOH·H_2O and HN^+Et_3·TsO^- are listed in Table S1. Strong basic and acidic solutions were obtained using NEt₃ and TsOH·H_2O, respectively. It should be noted that the pH value of the aqueous solution of the salt HN^+Et_3·TsO^- is 3.5. Since the salt is thermally stable up to 100 °C at least, the acidic salt catalyzes the polycondensation reaction of transesterified **1**.

To confirm the catalytic activity of HN^+Et_3·TsO^- for alkoxysilanes transesterified with 2-ME, polycondensation behavior of tris(2-methoxyethoxy)methylsilane (MeSi(ME)₃, room-temperature liquid) mixed with the catalysts was examined at 25 and 80 °C for 15 min (Table S2). Polycondensation of MeSi(ME)₃ was not promoted in the presence of triethylamine only. The mixtures containing TsOH·H_2O were hardened in spite of the reaction temperature, indicating the strong catalytic activity. It should be noted that the salt HN^+Et_3·TsO^- also catalyzed the polycondensation reaction of MeSi(ME)₃. This confirms that polycondensation of transesterified **1** is catalyzed by the salt in the TE/A method. Moreover, when the 1:10 mixture of TsOH·H_2O and NEt₃ was added to MeSi(ME)₃, polycondensation reaction did not proceed at 25 °C. That is, the acidic salt does not act as a catalyst in the

presence of an excess amount of basic NEt$_3$. This is the mechanism of the 'stop' of the polycondensation reaction. When NEt$_3$ is removed from the system by heating at 80–100 °C, the catalytic activity of the salt is restored and the sol–gel reaction is restarted (Table S2). MeSi(ME)$_3$ containing the acidic salt (HN$^+$Et$_3$·TsO$^-$) required 10–15 min to cure at room temperature under atmospheric exposure. In the TE/A method shown in Figs. 1 and 3, since the temperature was maintained at 80 °C, the polycondensation reaction proceeded rapidly, and the organosilica films were quickly cured in 1–3 min.

Table S1 Measured pH values of aqueous solutions containing 5 wt% of catalyst

Catalyst		pH
NEt$_3$		12.5
TsOH·H$_2$O		1.1
TsOH·H$_2$O/NEt$_3$ (molar ratio: 1/1)	$= HN^+Et_3·TsO^-$	3.5
TsOH·H$_2$O/NEt$_3$ (molar ratio: 1/10)	$= HN^+Et_3·TsO^-$ $+NEt_3$	11.9

Table S2 Observation of polycondensation behavior of MeSi(ME)$_3$ in the presence of various catalysts (4 wt%)

Catalyst	Reaction temperature (°C)	
	25	80
NEt$_3$	unhardened	unhardened
TsOH·H$_2$O	**hardened**	**hardened**
TsOH·H$_2$O/NEt$_3$ (molar ratio: 1/1)	**hardened**	**hardened**
TsOH·H$_2$O/NEt$_3$ (molar ratio: 1/10)	unhardened	**hardened**

To confirm the effect of basic compounds for suppressing the catalytic activity of the acids, we used amines with different basicities (triethylamine (pKa: 10.7), imidazole (pKa: 7.0) and pyridine (pKa: 5.3)). Organosilane precursor **1a** (90 mg) was transesterified using 2-ME (1.0 mL) and TsOH·H_2O (2 mg) at 130 °C for 15 min, and the mixture was cooled to room temperature. After adding pyridine (10 μL), imidazole (10 mg) or triethylamine (10 μL), the precursor solutions were spin-coated onto silicon wafers at 1500 rpm for 8 s and the curing times were measured at room temperature. The curing times were longer when stronger bases were used as shown in Table S3. This result indicates that the presence of a strong base is necessary to stop the hardening of the films.

Table S3 Curing times of transesterified **1a** in the TE/A method using different amine compounds at room temperature

Amine	pK_a	Curing time
pyridine	5.3	1−2 min
imidazole	7.0	10−15 min
triethylamine	10.7	~ 20 h

4. Supplementary data on metal oxide films

Fig. S14 shows the AFM image of the nanoimprinted TiO_2-TE/A and ZrO_2-TE/A films after calcination at 550 °C. In addition to those shown in Fig. 4, the nanoscale patterns formed on the surface of metal oxide films were retained after the calcination, although large volume shrinkage occurred to the films.
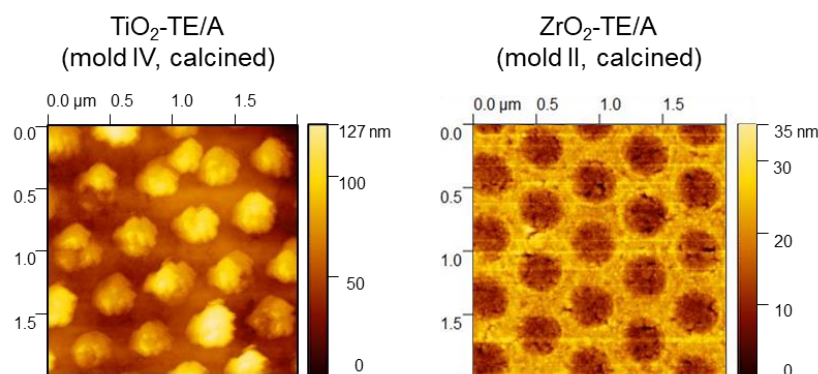

Fig. S14   AFM images of the nanoimprinted TiO_2-TE/A (mold IV) and ZrO_2-TE/A (mold II) films after calcination at 550 °C.

Fig. S15 shows FT-IR spectra of the metal oxide films before and after the calcination. In the FT-IR spectra of the films before calcination, absorption bands typical for alkyl groups (around 2900 cm^{-1}) are not observed, indicating most of the metal alkoxide groups disappeared by the heat treatment at 100 °C in the TE/A method. Small absorption peaks at 1200–1600 cm^{-1} are probably attributed to residual organic components. After the calcination, these peaks disappeared completely. The decreases of the broad absorption bands of M-OH groups (3000–3600 cm^{-1}) correspond to the polycondensation of the metal oxide frameworks.
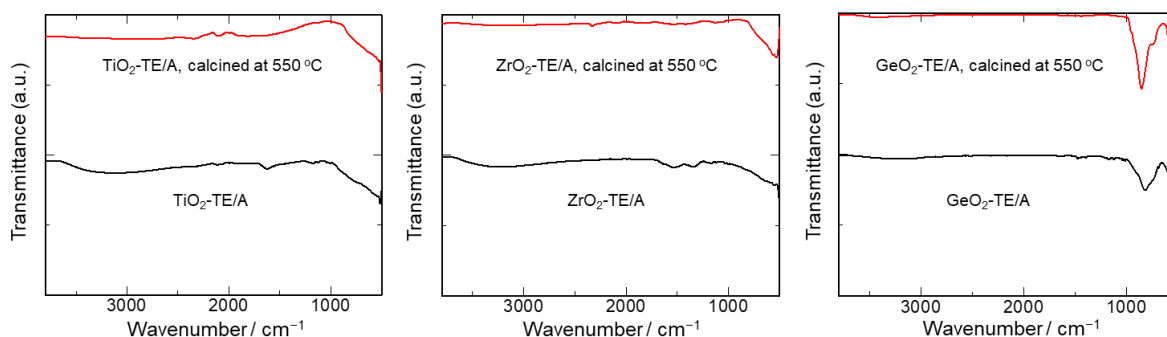

Fig. S15   FT-IR spectra of the metal oxide films prepared by the TE/A method (black) and those after calcination at 550 °C (red).

References

1   N. Mizoshita, Y. Yamada, M. Murase, Y. Goto and S. Inagaki, *Nanoscale*, 2020, **12**, 21146–21154.

2   N. Mizoshita, Y. Yamada, M. Murase, Y. Goto and S. Inagaki, *ACS Appl. Mater. Interfaces*, 2022, **14**, 3716–3725.

3   N. Mizoshita, M. Murase, Y. Yamada and Y. Goto, *Mater. Chem. Front.*, 2021, **5**, 851–861.

4   N. Mizoshita, T. Tani, H. Shinokubo and S. Inagaki, *Angew. Chem. Int. Ed.*, 2012, **51**, 1156–1160.